FULL PAPER DOI: 10.1002/adsc.202000082

Synthesis of Substituted 4-Arylamino-1,2-naphthoquinones in One-Pot Reactions Using CotA-Laccase as Biocatalyst

Ana Catarina Sousa,[a, b] Iolanda Santos,[a, b] M. F. M. M. Piedade,[b, c] Lígia O. Martins,[d,*] and M. Paula Robalo[a, b,*]

[a] Área Departamental de Engenharia Química, Instituto Superior de Engenharia de Lisboa, Instituto Politécnico de Lisboa, Rua Conselheiro Emídio Navarro, 1, 1959-007 Lisboa, Portugal
phone: +351218317163
E-mail: mprobalo@deq.isel.ipl.pt

[b] Centro de Química Estrutural, Complexo I, Instituto Superior Técnico, Universidade de Lisboa, Av. Rovisco Pais, 1049-001 Lisboa, Portugal

[c] Departamento de Química e Bioquímica, Faculdade de Ciências, Universidade de Lisboa, Campo Grande, 1649-016 Lisboa, Portugal

[d] Instituto de Tecnologia Química e Biológica, Universidade Nova de Lisboa, Av. da República, 2780-150 Oeiras, Portugal
phone: +351 214469534
E-mail: lmartins@itqb.unl.pt

Manuscript received: January 18, 2020; Revised manuscript received: April 4, 2020;
Version of record online: May 11, 2020

Supporting information for this article is available on the WWW under https://doi.org/10.1002/adsc.202000082

Abstract: An efficient and environmentally benign biocatalytic strategy for the synthesis of substituted 4-arylamino-1,2-naphthoquinones was developed, through a cross-coupling reaction in which the 1,2-naphthoquinone nucleus, formed in the biocatalytic process mediated by CotA-laccase from *Bacillus subtilis*, is the key synthetic intermediate. Electrochemical data and kinetic parameters were determined revealing a significant higher specificity of CotA-laccase for 4-amino-3-hydroxynaphthalene-1-sulfonic acid (AHNSA). This ability of CotA-laccase to discriminate between oxidisable aromatic amines allows the set-up of one-pot reactions in the presence of the enzyme, between AHNSA and a set of appropriate aromatic amines under mild reaction conditions.

Keywords: CotA-laccase; 4-arylamino-1,2-naphthoquinones; biocatalysis; green synthesis

Introduction

Naphthoquinones belong to a very important class of organic compounds in the pharmaceutical chemistry due to their unique redox and acid-base properties. Quinone cores are known to be electron transporters and quinone redox cycling, that yields "reactive oxygen species" (ROS), is important in many biological oxidative processes essential to living organisms.[1–5] Traditionally used due to their dyeing properties, more recently a variety of biological activities have been reported for naphthoquinones. The pharmacological profile of both natural and artificial naphthoquinones has been elucidated by numerous studies and a considerable number of naphthoquinone-based molecules with promising therapeutic potential have been identified.[1] Their chemical properties, intimately linked to their pharmacological activities are generally modulated by the different substituents (electron donors or acceptors) attached to the naphthoquinone core. The predominant scaffold in nature is the naphthalene 1,4-dione whose different derivatives have been highly explored as they display a wide spectrum of biological and pharmacological activities including anti-inflammatory, antibacterial, antitumour among other chemotherapeutic properties.[6–9] However, the less studied 1,2-dione isomers can also impart a key role in the development of new substances for medical purposes with a wide range of known derivatives exhibiting therapeutic properties as antitumour,[10–12] anti-inflammatory[13] and in other diseases like viral diseases[14] and diabetes.[15] Moreover, the incorporation of amino groups in the 1,2-naphthoquinone moiety

showed a positive contribution in the cytotoxic action of the compounds.[11]

The chemical synthesis of naphthoquinone derivatives is quite-well documented. Traditional protocols involve as first step the oxidation of the hydronaphthoquinone moiety with chemical oxidants such as H_2O_2, Fremy's salt [$(KSO_3)_2NO$], chromium trioxide and other oxidants[2,5] followed by the synthesis of the alkyl/arylaminonaphthoquinone derivatives described as a Michael 1,4-addition type reaction or a nucleophilic substitution of a mono- or dihalogenated naphthoquinone derivatives.[16] The use of organic solvents and aggressive chemical oxidants are not compatible with the increase need for more sustainable processes. Some other strategies include the use of natural naphthoquinones as starting materials, relying in their extraction from plants using extensive experimental procedures, tedious purification steps and considerable amounts of organic solvents.[17,18] Although there are some reports of environmentally friendly methodologies[3,19,20] such as ultrasonic or microwave assisted reactions, particularly directed towards 1,4-naphthoquinones synthesis, it remains a challenge to develop new sustainable synthetic routes for these compounds with lower environmental impact.

The increasing global demand for green strategies involving clean organic reactions brought notoriety to biocatalytic processes as powerful alternative tools in synthetic organic chemistry for fine chemicals manufacture. Enzyme-catalysed reactions offer several advantages compared to the traditional chemistry-catalysed reactions, in particular the use of aqueous reaction media, preventing the use of toxic and volatile organic solvents which became an environmental concern.[21–24]

Laccases (EC 1.10.3.2, *p*-diphenol:dioxygen oxidoreductases) are multicopper oxidoreductive enzymes which are versatile and efficient biocatalysts for the synthesis of different value-added chemicals and pharmaceuticals. Owing to their nontoxic nature, the use of oxygen as co-substrate and water as by-product, laccases are considered green catalysts in synthetic organic chemistry,[25] with reported examples for the synthesis of substituted 1,4-naphthoquinones.[26,27]

During the last years we have been exploring the oxidising abilities of CotA-laccase, from *Bacillus subtilis*,[28] for substituted aromatic amines looking for the development of sustainable organic protocols for access dyes and other compounds with potential biological activity. The aromatic amines play two different roles in laccase-catalysed reactions, as substrates leading to the correspondent imine intermediates and as nucleophilic partners in cross-coupling reactions with the previous intermediates.[29–32]

In the present work, we describe a clean, fast and simple method to obtain a family of substituted 4-phenylamine-1,2-naphthoquinones, mediated by CotA-laccase. In this procedure, the 1,2-naphthoquinone generated in situ from the oxidation of an aminonaphthol by laccase followed by hydrolysis, underwent the quinone reaction with the nucleophilic aromatic amine, being converted into the substituted 4-phenylamine-1,2-naphthoquinones. This biocatalytic process represents a new green approach for the preparation of the target molecules in short reaction times, at mild conditions, aqueous medium and room temperature.

Results and Discussion

The oxidation of 4-amino-3-hydroxynaphthalene-1-sulfonic acid (AHNSA, **1**, 5 mM) mediated by CotA-laccase (1 $U.mL^{-1}$) at pH 7 leads to the formation of the respective *ortho*-naphthoquinoneimine (**1 a**), which is further converted in the water soluble *ortho*-naphthoquinone (**1 b**) as presented in Scheme 1. The presence of the naphthalene scaffold is characterized by five signals in the aromatic region (6.7–8.5 ppm) and the *ortho*-quinone core confirmed by the presence of two characteristic carbon signals in the ^{13}C NMR at 181.6 and 178.4 ppm.

Considering the previous observations and mechanisms proposed[29,30,33] we can assume that CotA-laccase promotes the oxidation of substrate **1**, forming the respective *ortho*-naphthoquinoneimine intermediate (**1 a**), which suffers posterior hydrolysis at the terminal imine group under the aqueous reaction conditions, generating the 1,2-naphthoquinone core. In contrast to what has been observed in similar reactions with other substrates,[29,30] no further homocoupling reactions occurred, since the nucleophilic attack by another molecule is hampered by the substitution pattern of the aromatic rings, *e.g.* by the presence of substituents on the *para*-positions relative to the quinone groups. This unexpected result together with the absence of homocoupling reactions for product **1 b** prompted us to consider this compound as an appropriate candidate for heterocoupling reactions and prone to nucleophilic attack by other substituted anilines. In general, primary aromatic amines are good nucleophiles in water being their reactivity related with their structure.[33] Seven *p*-substituted anilines with different substituents, (see Scheme 2) mostly electron donor groups and cyano, an

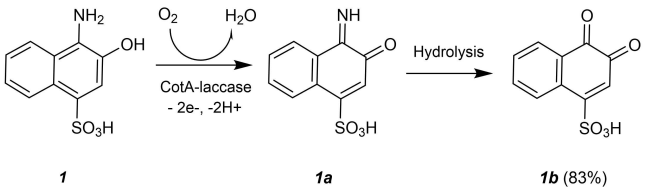

Scheme 1. Formation of *ortho*-naphthoquinone core **1 b** through the oxidation of 4-amino-3-hydroxynaphthalene-1-sulfonic acid mediated by CotA-laccase.

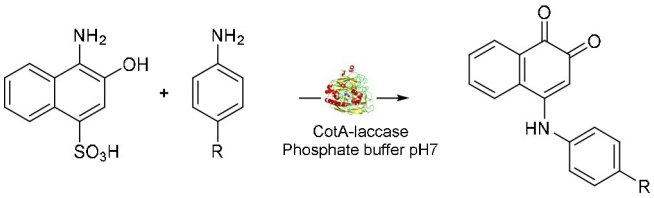

1	***2a*** (R = NH_2)	***3a*** (79 %)
	2b (R =OH)	***3b*** (80 %)
	2c (R = OCH_3)	***3c*** (78 %)
	2d (R = NHPh)	***3d*** (78 %)
	2e (R =$N(CH_3)_2$)	***3e*** (76 %)
	2f (R = $NHCOCH_3$)	***3f*** (71 %)
	2g (R = CN)	***3g*** (52 %)

Scheme 2. Synthetic route for 4-arylamine-1,2-naphthoquinone derivatives catalysed by CotA-laccase showing the products yields.

electron-withdrawing group, but with importance in pharmaceutical compounds[34] were chosen for potential nucleophilic partners. Some of these *p*-substituted aromatic amines with electron donor substituents are also substrates for CotA-laccase[35,36] and competitive reactions leading to a mixture of products can be expected. Therefore, the oxidation potential of AHNSA (**1**) and the kinetic parameters for CotA-laccase were determined and compared with the corresponding data previously obtained for amines **2 a**, **2 b**, **2 d** and **2 f**.[35] The oxidation potential (E_{pa}) was determined by cyclic voltammetry at pH 7 and a scan rate of 100 mV. s^{-1} and kinetic parameters were determined by non-linear-regression analysis at optimum pH. All data are summarised in Table 1.

The results indicated that all substrates, except 4-APA, showed lower E_{pa} values than the CotA-laccase (0.55 V *vs.* NHE)[37] indicating that at this respect they can be suitable substrates for the enzyme. Moreover, the redox potential (E_{pa}) for **1** is the lowest redox potential among the tested substrates suggesting a prioritised oxidation of **1** by the enzyme. The kinetic analysis showed that CotA-laccase exhibited a higher affinity (lower K_M) and a higher turn-over number (k_{cat}) for compound **1** ($K_M = 0.14$ mM and $k_{cat} = 36.7\ s^{-1}$), which resulted in a catalytic efficiency (k_{cat}/K_M) 10 to 300-fold higher when compared to the other primary aromatic amines. These results highlight the enzyme "favouritism" towards the oxidation of compound **1**, as compared to the recognised substrates **2 a**, **2 b**, **2 d** and **2 f**. The significantly higher catalytic efficiency for compound **1** together with the evidence of the formation of the *ortho*-naphthoquinone (**1 b**), suitable for nucleophilic attack, prompted us to perform cross-coupling reactions between compound **1** and the remaining aromatic amines, targeted at the synthesis of 4-arylamine-1,2-naphthoquinones derivatives. The final aim was to extend the scope of structural scaffolds formed by design using CotA-laccase.

The family of the 4-arylamine-1,2-naphthoquinones (**3 a**–**g**) was obtained from the cross-coupling reactions between AHNSA, **1** (5 mM) and the *p*-substituted anilines (**2 a**–**g**, 5 mM) in the presence of CotA-laccase (1 $U.mL^{-1}$) after 2 h, at pH 7 in an ethanol:phosphate buffer solution (1:9) and room temperature, as depicted in Scheme 2.

TLC analysis was used to monitor the time-course reactions and showed that they were completed in less than 2 h. The 4-arylamine-1,2-naphtoquinone derivatives (**3 a**–**g**) were isolated in moderated to good yields (52–80%). The nucleophilic capacity observed for all the *p*-substituted amines showed to be dependent on the electronic nature of the *p*-substituent that regulate the final yield of products, with enhanced nucleophilicity leading to higher yields.

Another notable result was the complete absence of the homocoupling products derived from the oxidation of the *p*-substituted anilines **2 a**–**2 f** previously described.[35,36] The enzymatic system showed high selectivity for the oxidation of AHNSA substrate. The close values for the oxidation potentials of all amines involved, with exception of 4-APA, cannot be considered as the responsible for the selectivity observed, which is most likely due to structural and conformational complementary between AHNSA and CotA. This ability to discriminate between different oxidisable substrates is herein reported to CotA-laccase for the first time.

Concerning the products characterisation, the ^{1}H-NMR spectra of all products (**3 a**–**g**) were very similar and exhibited comparable patterns, whose signals multiplicity was in accordance with the proposed

Table 1. Kinetic parameters of oxidation reactions catalysed by CotA-laccase at optimum pH and electrochemical data (in Britton-Robinson buffer).

Substrate	Optimum pH	K_M (mM)	k_{cat} (s^{-1})	k_{cat}/K_M ($mM^{-1}\ s^{-1}$)	E_{pa} (V) (at pH 7)	Reference
1	7	0.14 ± 0.04	36.7 ± 0.1	268.6 ± 0.1	0.37	This work
1,4-PDA (**2 a**)	7	0.6 ± 0.1	14.3 ± 0.5	23 ± 4.1	0.41	[35]
4-AP (**2 b**)	6	0.5 ± 0.1	2.2 ± 0.2	4 ± 0.8	0.40	[35]
4-ADA (**2 d**)	5	0.4 ± 0.1	14.3 ± 0.3	35 ± 4.0	0.44	[35]
4-APA (**2 f**)	7	1.3 ± 0.1	0.20 ± 0.04	0.10 ± 0.02	0.79	[35]

structures. The naphthalene scaffold is defined by five signals, two duplets and two triplets, in the aromatic range (δ = 7.48–8.40 ppm) and one singlet (δ = 5.54–6.30 ppm) for which is evident the shielding effect caused by the quinone nucleus. The amine substituent is characterised by two duplets with resonances in the aromatic region (δ = 6.83–7.89 ppm). The observed patterns suggest that the heterocoupling products resulted from the formation of a N–C bond in the occupied position of the quinone ring instead of a free position. Based on this evidence the displacement of the sulfonyl group was predicted and later confirmed by electrospray ionisation (ESI) (negative and positive ion modes) mass spectrometry measurements followed by tandem experiments. The mass spectra of products **3a**, **3b**, **3c**, **3d** and **3f** exhibited signals at *m/z* 265, 266, 280, 341, 293 and 307, correspondent to the protonated molecules $[M+H]^+$ while **3g** was detected in negative mode with *m/z* 273 for $[M-H]^-$. The fragmentation of the previous ions yielded mainly the fragment ions of *m/z* 237, 238, 279, 252, 313, 265, 245 respectively, in concordance with the loss of a CO molecule. Further fragmentation, namely MS^3 experiments showed for most of the compounds (**3a**, **3b**, **3d**, **3f** and **3g**) a second loss of an additional CO molecule, consistent with the presence of two carbonyl groups in the final products.

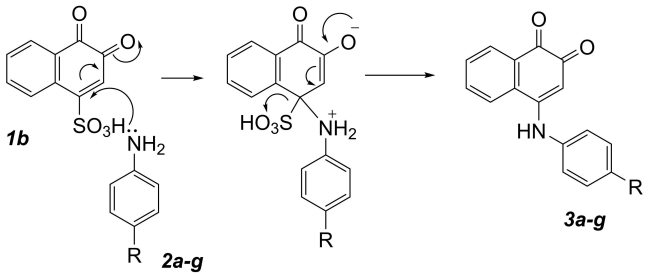

Scheme 3. Proposed mechanism for the formation of 4-arylamine-1,2-naphthoquinone derivatives.

A plausible mechanism for the formation of the target molecules is presented in Scheme 3 where the *ortho*-naphthoquinone intermediate (**1b**), generated in situ by CotA-laccase oxidation of 4-amino-3-hydroxynaphthalene-1-sulfonic acid (**1**), suffers nucleophilic attack on the C1 position (the carbon bearing the sulfonyl leaving group) by the aromatic amines (**2a–g**) to give an enolate intermediate. This species undergoes subsequent displacement of the sulfonyl group leading to the formation of the 4-arylamine-1,2-naphtoquinones products (**3a–g**).

Crystals of product **3b** were obtained by slow evaporation of an ethanol solution and single crystal X-ray analysis was performed at room temperature. Compound **3b** is triclinic, crystallises in space group P-1 with two independent molecules in the asymmetric unit. The molecular diagram of compound **3b** is shown in Figure 1A with the label scheme.

The molecules are not planar with an angle of 49.8° (60.6° for molecule A) between the planes of the aminophenol substituent and the naphthalene core. The most noticiable feature in the crystalline packing of this compound is the synthon $R^2_4(18)$ formed by 4 molecules through the hydrogen bonds of the type O–H…O and a bifurcated one of the type N–H…O (for aminophenol substituent and the naphthalene core. distances see Table S2 of SI) (Figure 2). This synthon is reinforced by two other O–H…O hydrogen bonds (in orange in Figure 2). This building block is propagated along the [111] plane leading to the overall molecular packing of this compound.

Conclusion

The present work describes a new simple and eco-friendly approach for the synthesis of substituted 4-arylamine-1,2-naphthoquinones via one-pot reaction using CotA-laccase as biocatalyst to promote the oxidation of 4-amino-3-hydroxynaphthalene-1-sulfonic acid and 4-substituted arylamines. This oxidative

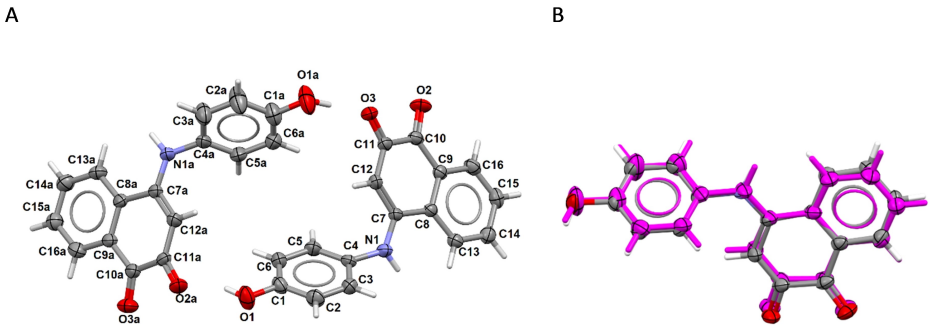

Figure 1. A) Molecular diagrams of the two inequivalent molecules, with the label scheme. The ellipsoids were drawn at 50% probability; B) overlap of the two molecules in the asymmetric unit.

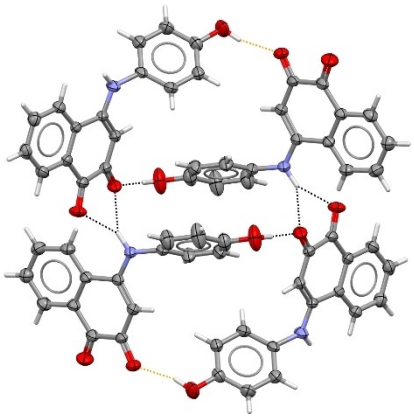

Figure 2. $R^2_4(18)$ synthon formed by hydrogen bonds of the type O–H…O and N–H…O. In orange two O–H…O hydrogen bondsreinforcing the ring.

strategy promotes the formation of the cross-coupling products with high yields (52 to 80%) in aqueous medium using aerial oxygen, in less than 2 hours. The ability to discriminate between oxidisable substrates observed, for the first time, for this enzyme allowed the design of new molecules only based on the nucleophilic power of the aromatic amines. The formation of this new class of compounds broadens the competences of CotA-laccase as biocatalyst and opens new perspectives for its use in organic synthesis, particularly in the area of fine chemicals synthesis.

Experimental Section

General Experimental Information

All reagents and solvents are commercially available, purchased with high purity from Sigma-Aldrich and Alfa Aesar and used without further purification. Reactions were monitored by thin layer chromatography (TLC) on aluminum sheets pre-coated with silica gel Merck 60 F254. Column chromatography was carried out using silica gel 60 (EM Separations Technology) as the stationary phase. Melting points were determined with an Electrothermal 9100 digital melting point apparatus. NMR spectra were recorded on a Bruker Avance (400 MHz) spectrometer in CD_3OD-d_4 and DMSO-d_6 as solvents with a 5 mm probe. Spectra were referenced to the residual ^1H signal of the deuterated solvent. The following abbreviations are used in reporting the NMR data: s (singlet), d (doublet), t (triplet) and m (multiplet)). Coupling constants (J) are in Hz. Spectra are reported as follows: chemical shift (δ, ppm), multiplicity, integration, coupling constants (Hz).

Low resolution mass spectra were recorded on a LCQ Fleet, Thermo Scientific Ion Trap mass spectrometer, operated in the electrospray ionisation (ESI) positive/negative ion modes. The optimised parameters were as following: ion spray voltage, ±4.5 kV; capillary voltage, +16 and −20 V; tube lens offset, −63 and +82 V; sheath gas (N_2), 80 arbitrary units; auxiliary gas, 5 arbitrary units; capillary temperature, 250 °C. The spectra were recorded in the range 50–1000 Da. Spectrum typically corresponds to the average of 20–35 scans. Sequential mass spectra was obtained with an isolation window of 2 Da, a 25–30% relative collision energy and with an activation energy of 30 msec. High Resolution ESI(+/-) mass spectra were obtained on a QTOF Impact IITM mass spectrometer (Bruker Daltonics, GMBH; Germany), operating in the high resolution ion mode. Calibration of the TOF analyser was performed with a 10 mM sodium formate calibrant solution. Data was processed using Data Analysis 4.2 software.

The redox potentials were measured by cyclic voltammetry using an EG&G Princeton Applied Research (PAR) Model 273A potentiostat/galvanostat monitored with the Electrochemistry PowerSuite v2.51 software from PAR. Cyclic voltammograms were obtained in 1 mM of substrates in phosphate buffer (20 mM):ethanol (9:1) solutions, using a three electrode configuration cell with an home-made platinum disk working electrode (1.0 mm diameter), a platinum wire counter electrode and an Ag/AgCl reference electrode (purchased from Radiometer analytical, SAS, France). The potential was scanned from −0.7 to 1.2 V at a scan rate of 100 $mV.s^{-1}$. All measurements were done at room temperature and the solutions were deaerated with dinitrogen. The measured potentials were corrected by +0.197 V to the normal hydrogen electrode (NHE).

Production and Purification of CotA-Laccase

Recombinant CotA-laccase from *Bacillus subtilis* was produced and purified as previously described.[28,37,38] The oxidation of ABTS was followed by an absorbance increase at 420 nm ($\varepsilon = 3.6 \times 10^4\ M^{-1}.cm^{-1}$). The protein concentration was measured using the Bradford assay[39] and bovine serum albumin was used as a standard. One unit (U) of enzymatic activity was defined as the amount of enzyme that transformed 1 µmol of ABTS per min at 37 °C.

Kinetic Parameters of CotA-Laccase

The enzymatic reactions with compound **1** (in the concentration range 0.005–5 mM) were performed at 37 °C at the optimal pH (in Britton & Robinson buffer, pH 7) and were monitored at 400 nm ($\varepsilon = 605\ M^{-1}.cm^{-1}$). For the other substrates, the enzymatic reactions were monitored at 510 nm ($\varepsilon = 3{,}467\ M^{-1}.cm^{-1}$), 400 nm ($\varepsilon = 9{,}551\ M^{-1}.cm^{-1}$), 570 nm ($\varepsilon = 1{,}046\ M^{-1}.cm^{-1}$) and 360 nm ($\varepsilon = 8{,}335\ M^{-1}.cm^{-1}$) for compounds **2a**, **2b**, **2d** an **2f** respectively, as previously described.[35] Kinetic constants (K_M and k_{cat}) were fitted directly to Michaelis-Menten equation (OriginLab software, North-Ampton, MS, USA). All enzymatic assays were performed at least in triplicate.

Enzymatic Oxidation of 4-Amino-3-hydroxynaphthalene-1-sulfonic acid

4-amino-3-hydroxynaphthalene-1-sulfonic acid (12.0 mg, 0.05 mmol) was dissolved in 10 mL of 20 mM phosphate buffer pH 7. Reactions were started by adding 1 $U.mL^{-1}$ of CotA-laccase. The resulting orange mixture was stirred at room temperature, under aerobic conditions and the reaction was monitored by TLC until disappearance of the starting material. Once the reaction was completed, the solvent was evaporated

under reduced pressure. Purification was accomplished by column chromatography on silica gel and eluted with a mixture of ethyl acetate:hexane (3:1). Product **1 b** was obtained as an orange solid with a yield of 83%.

4-(Sulfonic)naphtalene-1,2-dione (1 b): Orange solid; yield: (9.7 mg, 83%); ^{1}H RMN (400 MHz, DMSO-d_6): δ (ppm) = 8.41 (d, 1H, J = 8.9 Hz, H_5), 7.95 (d, 1H, J = 8.9 Hz, H_8), 7.73 (t, 1H, J = 8.4 Hz, H_6), 7.55 (t, 1H, J = 8.4 Hz, H_7), 6.73 (s, 1H, H_3). ^{13}C NMR (DMSO-d_6) δ (ppm) = 181.6 (C2), 178.4 (C1), 156.5 (C4), 134.4 (C6), 131.9 (C10), 131.7 (C9), 130.5 (C5), 129.9 (C7), 128.8 (C8), 124.1 (C3). ESI/MS negative mode: *m/z* 237 $[M-H]^-$; MS^2 m/z 173 $[M-H-SO_2]^-$; MS^3 145 $[M-H-SO_2-CO]^-$.

General Procedure for the Cross-Coupling Reactions

4-amino-3-hydroxynaphthalene-1-sulfonic acid (12 mg, 0.05 mmol) and the different aromatic amines (**2 a–g**) (0.05 mmol) were dissolved in 10 mL of an ethanol: 20 mM phosphate buffer (pH 7) solution (1:9) in a 25 mL round-bottom flask. After the solubilisation of the starting materials, 1 U. mL^{-1} of CotA-laccase was added and an immediate change of colour was observed in all assays. Reactions proceed with stirring, at room temperature, under aerobic conditions and progress was monitored by TLC. The final products were isolated by filtration or by extraction with ethyl acetate followed by solvent removal. Whenever necessary the crude residues were purified by preparative/column chromatography.

Characterization of the 4-Arylamino-1,2-naphthoquino- ne Products

4-(Aminophenylamino)naphthalene-1,2-dione (3 a)

Purple solid (10.2 mg, 79%), mp = 212.0–212.9 °C. ^{1}H NMR (400 MHz, CD_3OD-d_4): δ (ppm) = 8.19 (d, 1H, *J* = 8.8 Hz, H5), 8.16 (d, 1H, *J* = 7.6 Hz, H8), 7.83 (t, 1H, *J* = 8.8 Hz, H6), 7.73 (t, 1H, *J* = 8.8 Hz, H7), 7.10 (d, 2H, *J* = 8.8 Hz, H12,16), 6.83 (d, 2H, *J* = 8.8 Hz, H13,15) and 5.92 (s, 1H, H3). ^{13}C NMR (DMSO-d_6) δ(ppm) = 181.8 (C1), 175.2 (C2), 155.0 (C4), 148.0 (C14), 134.2 (C6), 131.4 (C7), 130.7 (C10), 130.6 (C9),128.0 (C8), 127.1 (C12,16), 125.4 (C11), 123.6 (C5), 114.1 (C13,15), 99.8 (C3). UV/Vis: 500 nm, ε = 2 428 $M^{-1}cm^{-1}$ (ethanol). ESI-MS positive mode: 287 $[M+Na]^+$; 265 $[M+H]^+$, MS^2 (*m/z*): 237 $[M+H-CO]^+$, MS^3 (*m/z*): 209 $[M+H-CO-CO]^+$; ESI-MS negative mode: 263 $[M-H]^-$. ESI-HRMS: *m/z* calcd. for $[C_{16}H_{13}N_2O_2+H]^+$: 265.0972; found 265.0974.

4-(Hydroxyphenylamino)naphtalene-1,2-dione (3 b)

Red solid (10.6 mg, 80%), mp = 310.7–311.2 °C. ^{1}H NMR (400 MHz CD_3OD-d_4): δ (ppm) = 8.22 (d, 1H, J = 7.6 Hz, H5), 8.14 (d, 1H, *J* = 7.2 Hz, H8), 7.80 (t, 1H, J = 7.2 Hz, H6), 7.70 (t, 1H, *J* = 7.2 Hz, H7), 7.12 (d, 2H, *J* = 8.0 Hz, H12,16), 6.90 (d, 2H, J = 8.4 Hz, H13,15) and 5.91 (s, 1H, H3). ^{13}C NMR (DMSO-d_6) δ(ppm) = 181.5 (C1), 175.4 (C2), 156.4 (C4), 155.1 (C14), 134.3 (C6), 131.5 (C7), 131.4 (C10), 130.8 (C9), 128.7 (C8), 128.1 (C11), 127.7 (C12,16), 123.7 (C5), 116.0 (C13,15) and 99.9 (C3). UV/Vis: 480 nm, ε = 4 936 $M^{-1}cm^{-1}$ (Ethanol). ESI-MS positive mode: 288 $[M+Na]^+$; 266 $[M+H]^+$, MS^2 (*m/z*): 238 $[M+H-CO]^+$, MS^3 (*m/z*): 210 $[M+H-CO-CO]^+$; ESI-MS negative mode: 264 $[M-H]^-$. ESI-HRMS: *m/z* calcd. for $[C_{16}H_{11}NO_3+H]^+$: 266.0812; found 266.0810.

4-(Methoxyphenylamino)naphtalene-1,2-dione (3 c)

Dark red solid (10.9 mg, 78%), mp = 249.8–250.4 °C. ^{1}H NMR (400 MHz, DMSO-d_6): δ (ppm) = 9.82 (bs, 1H, NH), 8.31 (bs, 1H, H5), 8.04 (d, 1H, J = 8.0 Hz, H8), 7.87 (t, 1H, *J* = 7.6 Hz, H6), 7.74 (t, 1H, *J* = 7.6 Hz, H7), 7.31 (bs, 2H, H12,16), 7.07 (d, 2H, *J* = 8.4 Hz, H13,15), 5.54 (s, 1H, H3) and 3.81 (s, 3H, CH_3). ^{13}C NMR (DMSO-d_6) δ (ppm) = 181.2 (C1), 175.4 (C2), 158.0 (C14), 154.9 (C4), 134.0 (C6), 131.5 (C7), 131.2 (C10), 131.1 (C9), 130.5 (C11), 128.1 (C8), 127.6 (C12,16), 123.8 (C5), 114.7 (C13,15), 99.8 (C3) and 55.3 (CH_3). UV/Vis: 475 nm, ε = 5 389 $M^{-1}cm^{-1}$ (Ethanol). ESI-MS positive mode: 280 $[M+H]^+$, MS^2 (*m/z*): 252 $[M+H-CO]^+$; ESI-MS negative mode: 278 $[M-H]^-$.ESI-HRMS: *m/z* calcd. for $[C_{17}H_{13}NO_3+H]^+$: 280.0968; found 280.0969.

4-(Aminodiphenylamino)naphtalene-1,2-dione (3 d)

Purple solid (13.3 mg, 78%), mp = 247.6–248.2 °C. ^{1}H NMR (400 MHz, DMSO-d_6): δ (ppm) = 9.91 (bs, 1H, NH), 8,39 (s, 1H, NH), 8.33 (d, 1H, *J* = 7.9 Hz, H5), 8.04 (d, 1H, *J* = 7.7 Hz, H8), 7.86 (t, 1H, *J* = 7.6 Hz, H6), 7.73 (t, 1H, *J* = 7.5 Hz, H7), 7.27 (t, 2H, J = 7.7 Hz, H19,21), 7.18 (s, 4H, H13,15,18,22), 7.13 (d, 2H, *J* = 7.9 Hz, H12,16), 6.87 (t, 1H, *J* = 7.3 Hz, H20) and 5.81 (bs, 1H, H3). ^{13}C NMR (DMSO-d_6) δ (ppm) = 181.4 (C1), 154.6 (C4), 142.9 (C14,17), 134.1 (C6), 131.4 (C7), 131.2 (C9,10), 129.3 (C12,16,19,21), 127.6 (C8), 123.8 (C5), 120.2 (C20), 117.2 (C11,18,22), 116.7 (C13,15) and 100.6 (C3). UV/Vis: 520 nm, ε = 4 979 $M^{-1}cm^{-1}$ (Ethanol). ESI-MS positive mode: 341 $[M+H]^+$, MS^2 (*m/z*): 313 $[M+H-CO]^+$, ESI-MS negative mode: 339 $[M-H]^-$; MS^2 (*m/z*): 311 $[M-H-CO]^-$, MS^3 (*m/z*): 283 $[M-H-CO-CO]^-$. ESI-HRMS: *m/z* calcd. for $[C_{22}H_{15}N_2O_2+H]^+$: 341.1285; found 341.1279.

4-(Dimethylphenylamino)naphtalene-1,2-dione (3 e)

Dark purple solid (11.1 mg, 76%), mp = 215.3–216.0 °C. ^{1}H NMR (400 MHz, DMSO-d_6): δ (ppm) = 8.04 (bs, 1H, H5), 7.72 (bs, 1H, H8), 7.62 (bs, 1H, H6), 7.48 (d, 1H, *J* = 7.8 Hz, H7), 7.40 (d, 2H, *J* = 8.3 Hz, H12,16), 6.85 (d, 2H, *J* = 8.3 Hz, H13,15), 6.30 (s, 1H, H3) and 3.01 (s, 6H, CH_3).^{13}C NMR (DMSO-d_6) δ(ppm) = 179.5 (C1), 179.4 (C2), 155.7 (C4), 151.4 (C14), 134.8 (C8), 134.7 (C10), 132.0 (C9), 130.6 (C6), 129.8 (C12,16), 129.4 (C7), 129.3 (C5), 125.5 (C3), 122.9 (C11), 111.8 (C13,15) and 40.0 (CH_3, under the solvent peak). UV/Vis: 525 nm, ε = 6 529 $M^{-1}cm^{-1}$ (Ethanol). ESI-MS positive mode: 293$[M+H]^+$, MS^2 (*m/z*): 265 $[M+H-CO]^+$, ESI-HRMS: *m/z* calcd. for $[C_{18}H_{16}N_2O_2+H]^+$: 293.1285; found 293.1283.

4-(Acetaminophenylamino)naphtalene-1,2-dione (3 f)

Dark red solid (10.8 mg, 71%), mp = 349.9–350.3 °C. ^{1}H NMR (400 MHz, DMSO-d_6): δ (ppm) = 10.08 (s, 1H, NH), 9.88 (bs, 1H, NH), 8.30 (d, 1H, *J* = 6.9 Hz, H5), 8.02 (d, 1H, *J* = 6.9 Hz, H8), 7.84 (bs, 1H, H6), 7.77–7.60 (m, 3H, H7, H13,15), 7.20

(bs, 2H, H12,16), 5.73 (bs, 1H, H3) and 2.05 (s, 3H, CH_3). ^{13}C NMR (DMSO-d_6) δ (ppm) = 181.2 (C1), 168.6 (C=O), 154.7 (C4), 134.1 (C6), 131.5 (C7), 131.2 (C9,10), 128.4 (C8), 126.7 (C12,16), 123.9 (C5), 119.6 (C11,13,15) and 23.8 (CH_3). UV/Vis: 465 nm, ε = 4 456 $M^{-1}cm^{-1}$ (Ethanol). ESI-MS positive mode: 307$[M+H]^+$, MS^2 (*m/z*): 279 $[M+H–CO]^+$, MS^3 (*m/z*): 251 $[M+H–CO–CO]^+$. ESI-HRMS: *m/z* calcd. for $[C_{18}H_{14}N_2O_3+H]^+$: 307.1077; found 307.1078.

4-(Cyanophenylamino)naphtalene-1,2-dione (3g)

Red solid (7.1 mg, 52%), mp = 250.3–250.8 °C. ^1H NMR (300 MHz, DMSO-d_6): δ(ppm) = 8.31 (d, 1H, J = 7.8 Hz, H5), 8.06 (d, 1H, J = 7.8 Hz, H8), 7.89 (d, 2H, J = 7.8 Hz, H13,15), 7.83 (m, 1H, J = 7.2 Hz, H6), 7.73 (t, 1H, J = 7.8 Hz, H7), 7.24 (d, 2H, J = 8.4 Hz, H12,16) and 6.03 (s, 1H, H3). ^{13}C NMR (DMSO-d_6) δ (ppm) = 181.2 (C1), 181.1 (C2), 154.4 (C4), 144.2 (C11), 133.9 (C13,15), 133.7 (C6), 132.1 (C9), 131.7 (C7), 131.2 (C10), 126.8 (C8), 125.6 (C5), 121.7 (C12,16), 119.5 (CN), 105.3 (C14) and 100.3 (C3). UV/Vis: 457 nm, ε = 3 411 $M^{-1}cm^{-1}$ (Ethanol). ESI-MS negative mode: 273 $[M-H]^-$; MS^2 (*m/z*): 245 $[M-H–CO]^-$, MS^3 (*m/z*): 217 $[M-H–CO–CO]^-$. ESI-HRMS: *m/z* calcd. for $[C_{17}H_{10}N_2O_2–H]^-$: 341.1285; found 341.1279.

X-Ray Crystal Structural Data

Crystals suitable for X-ray analysis were obtained by slow evaporation of saturated solution in ethanol. The crystal was mounted on a loop with Fomblin protective oil and the X-ray data was collected at room temperature on a Bruker AXS-KAPPA APEX II diffractometer with graphite monochromated radiation (Mo Kα, λ = 0.71069 Å) with the generator operating at 50 kV and 30 mA. Data were corrected for Lorentzian, polarization, and absorption effects using SAINT[40] and SADABS[41] programs. The structure was solved by the Intrinsic Phasing methods using SHELXT-2014[42] incorporated in the Bruker diffractometer interface. SHELXL-2017/1,[42] included in the program package WINGX-Version 2014.1[43] was used for refinement using full matrix least-squares on F2. A full-matrix least-squares refinement was used for the non-hydrogen atoms with anisotropic thermal parameters. All the hydrogens were inserted in idealised positions and allowed to refine riding in the parent carbon atom, except the hydrogens that are bonded to the nitrogen and oxygen atoms that were found in the electron density map. The graphics were made using MERCURY 3.0.[44] PLATON[45] was used for hydrogen bond and intermolecular interactions. Table S1 of SI summarises crystallographic details for compound **3b**. The hydrogen bond distances and angles are included in Table S2. CCDC 1967820 contains the Cif file for this compound. These data can be obtained free of charge from The Cambridge Crystallographic Data Centre via http://www.ccdc.cam.ac.uk

Acknowledgements

This work was supported by FCT – Fundação para a Ciência e Tecnologia through projects PTDC/BIO/72108/2006, PTDC/BBB-EBB/0122/2014, RECI/QEQ-QIN/0189/2012 and REM2013 and R&D units UID/QUI/00100/2019 and UID/Multi/04551/2013 (GreenIT). The authors thank Dr M. Conceição Oliveira for the helpful discussions about the ESI-MS results and the IST-UL NMR Network for facilities.

References

[1] H. Y. Qiu, P. F. Wang, H. Y. Lin, C. Y. Tang, H. L. Zhu, Y. H. Yang, *Chem. Biol. Drug Des.* **2018**, *91*, 681–690.
[2] J. López, F. de la Cruz, Y. Alcaraz, F. Delgado, M. A. Vázquez, *Med. Chem. Res.* **2015**, *24*, 3599–3620.
[3] L. Ramos-Peralta, L. I. López-López, S. Y. Silva-Belmares, A. Zugasti-Cruz, R. Rodríguez-Herrera, C. N. Aguilar-González, in " *The Battle Against Microbial Pathogens: Basic Science, Technological Advances and Educational Programs*", ed. A. Méndez-Vilas, Formatex Microbiology Series n° 5, Formatex Research Center, Badajoz, Spain, **2015**, vol. 1, 542–550.
[4] Y. Kumagai, Y. Shinkai, T. Miura, A. K. Cho, *Annu. Rev. Pharmacol. Toxicol.* **2012**, *52*, 221–247.
[5] V. K. Tandon, S. Kumar, *Expert Opin. Ther. Pat.* **2013**, *23*, 1087–1108.
[6] V. P. Papageorgiou, A. N. Assimopoulou, E. A. Couladouros, D. Hepwort, K. C. Nicolaou, *Angew. Chem. Int. Ed.*, **1999**, *38*, 270–301.
[7] M. Janeczko, O. M. Demchuk, D. Strzelecka, K. Kubinski, M. Masłyk, *Eur. J. Med. Chem.* **2016**, *124*, 1019–1025.
[8] a) J. C. R. Gonçalves, T. H. Coulidiati, A. L. Monteiro, L. C. T. C. Gonçalves, W. O. Valença, R. N. Oliveira, C. A. Câmara, D. A. M. Araújo, *J. Appl. Biomed.* **2016**, *14*, 229–244; b) S. Fiorito, S. Genovese, V. A. Taddeo, V. Mathieu, R. Kiss, F. Epifano, *Bioorg. Med. Chem. Lett.* **2016**, *26*, 334–337; c) M. Kubanik, W. Kandioller, K. Kim, R. F. Anderson, E. Klapproth, M. A. Jakupec, A. Roller, T. Söhnel, B. K. Keppler, C. G. Hartinger, *Dalton Trans.* **2016**, *45*, 13091–13103.
[9] S. H. Cardoso, C. R. Oliveira, A. S. Guimarães, J. Nascimento, J. O. S. Carmo, J. N. S. Ferro, A. C. C. Correia, E. Barreto, *Chem.-Biol. Interact.* **2018**, *291*, 55–66.
[10] L. Wu, *RSC Adv.* **2015**, *5*, 24960–24965.
[11] S. Shulkla, R. S. Srivastava, S. K. Shrivastava, A. Sodhi, P. Kumar, *Appl. Biochem. Biotechnol.* **2012**, *167*, 1430–1445.
[12] M. J. Hatfield, J. Chen, E. M. Fratt, L. Chi, J. C. Bollinger, R. J. Binder, J. Bowling, J. L. Hyatt, J. Scarborough, C. Jeffries, P. M. Potter, *J. Med. Chem.* **2017**, *60*, 1568–1579.
[13] C. H. Tseng, C. M. Cheng, C. C. Tzeng, S. I. Peng, C. L. Yang, Y. L. Chen, *Bioorg. Med. Chem.* **2013**, *21*, 523–531.
[14] F. J. Bullock, J. F. Tweedie, D. D. McRitchie, M. A. Tucker, *J. Med. Chem.* **1970**, *13*, 97–103.
[15] J. H. Ahn, S. Y. Cho, J. D. Ha, S. Y. Chu, S. H. Jung, Y. S. Jung, J. Y. Baek, I. K. Choi, E. Y. Shin, S. K. Kang, S. S. Kim, H. G. Cheon, S. D. Yang, J. K. Choi, *Bioorg. Med. Chem. Lett.* **2002**, *12*, 1941–1946.
[16] A. A. Kutyrev, *Tetrahedron* **1991**, *47*, 8043–8065.

[17] a) G. A. M. Jardim, T. T. Guimarães, M. C. F. R. Pinto, B. C. Cavalcanti, K. M. Farias, C. Pessoa, C. C. Gatto, D. K. Nair, I. N. N. Namboothiri, E. N. Silva Jr, *MedChemComm* **2015**, *6*, 120–130; b) E. N. Silva Júnior, I. M. M. Melo, E. B. T. Diogo, V. A. Costa, J. D. Souza Filho, W. O. Valença, C. A. Camara, R. N. Oliveira, A. S. Araujo, F. S. Emery, M. R. Santos, C. A. Simone, R. F. S. Menna-Barreto, S. L. Castro, *Eur. J. Med. Chem.* **2012**, *52*, 304–321.
[18] K. Mathiyazhagan, A. Kumara, P. Arjun, *Russ. J. Bioorg. Chem.* **2018**, *44*, 346–353.
[19] a) E. Leyva, A. Cárdenas-Chaparro, S. E. Loredo-Carrillo, L. I. López, F. Méndez-Sánchez, A. Martínez-Richa, *Mol. Diversity* **2018**, *22*, 281–290; b) L. I. López-López, J. J. V. Garcia, A. Sáenz-Galindo, S. Y. Silva-Belmares, *Lett. Org. Chem.* **2014**, *11*, 573–582.
[20] L. J. Mitchell, W. Lewis, C. J. Moody, *Green Chem.* **2013**, *15*, 2830–2833.
[21] R. A. Sheldon, J. M. Woodle, *Chem. Rev.* **2018**, *118*, 801–838.
[22] M. D. Truppo, *ACS Med. Chem. Lett.* **2017**, *8*, 476–480.
[23] A. Illanes in *White Biotechnology for Sustainable Chemistry*, Green Chemistry Series, (Eds.: M. A. Coelho, B. D. Ribeiro), Royal Society of Chemistry, Cambridge, **2015**, chap. 3, pp. 36–51.
[24] C. M. Clouthier, J. N. Pelletier, *Chem. Soc. Rev.* **2012**, *41*, 1585–1605.
[25] a) M. D. Cannatelli, A. J. Ragauskas, *Chem. Rec.* **2017**, *17*, 122; b) T. Kudanga, L. Nemadziva, M. Le Roes-Hill, *Appl. Microbiol. Biotechnol.* **2017**, *101*, 13–33; c) C. Romero-Guido, A. Baez, E. Torres, *Catalysts* **2018**, *8*, 223–244; d) M. Mogharabi, M. A. Faramarzi, *Adv. Synth. Catal.* **2014**, *356*, 897–927.
[26] S. Witayakran, A. J. Ragauskas, *Green Chem.* **2007**, *9*, 475–480.
[27] a) K. W. Wellington, R. Bokako, N. Raseroka, P. Steenkamp, *Green Chem.* **2012**, *14*, 2567–2576; b) K. W. Wellington, N. I. Kolesnikova, *Bioorg. Med. Chem.* **2012**, *20*, 4472–4481.
[28] L. O. Martins, C. M. Soares, M. M. Pereira, M. Teixeira, G. H. Jones, A. O. Henriques, *J. Biol. Chem.* **2002**, *277*, 18849–18859.
[29] A. C. Sousa, M. C. Oliveira, L. O. Martins, M. P. Robalo, *Adv. Synth. Catal.* **2018**, *360*, 575–583.
[30] A. C. Sousa, M. C. Oliveira, L. O. Martins, M. P. Robalo, *Green Chem.* **2014**, *16*, 4127–4136.
[31] A. C. Sousa, M. F. M. M. Piedade, L. O. Martins, M. P. Robalo, *Green Chem.* **2015**, *17*, 1492–1433.
[32] A. C. Sousa, M. F. M. M. Piedade, L. O. Martins, M. P. Robalo, *Green Chem.* **2016**, *18*, 6063–6070.
[33] F. Bruyneel, O. Payen, A. Rescigno, B. Tinant, J. Marchand-Brynaert, *Chem. Eur. J.* **2009**, *15*, 8283–8295.
[34] a) Y. Wang, Y. Du, N. Huang, *Future Med. Chem.* **2018**, *10*, 2713–2728; b) F. F. Fleming, L. Yao, P. C. Ravikumar, L. Funk, B. C. Shook, *J. Med. Chem.* **2010**, *53*, 7902–7917.
[35] A. C. Sousa, L. O. Martins, M. P. Robalo, *Adv. Synth. Catal.* **2013**, *355*, 2908–2917.
[36] A. C. Sousa, S. R. Baptista, L. O. Martins, M. P. Robalo, *Chem. Asian J.* **2019**, *14*, 187–193.
[37] P. Durão, Z. Chen, A. T. Fernandes, P. Hildebrandt, D. H. Murgida, S. Todorovic, M. M. Pereira, E. P. Melo, L. O. Martins, *J. Biol. Inorg. Chem.* **2008**, *13*, 183–193.
[38] I. Bento, L. O. Martins, G. G. Lopes, M. A. Carrondo, P. F. Lindley, *Dalton Trans.* **2005**, 3507–3513.
[39] M. Bradford, *Anal. Biochem.* **1976**, *72*, 248–254.
[40] SAINT+, release 6.22; Bruker Analytical Systems: Madison,WI, **2005**.
[41] SADABS; Bruker Analytical Systems: Madison,WI, **2005**.
[42] G. M. Sheldrick, *Acta Crystallogr. Sect. A* **2015**, *71*, 3–8.
[43] L. J. Farrugia, *J. Appl. Crystallogr.* **1999**, *32*, 837–838.
[44] C. F. Macrae, I. J. Bruno, J. A. Chisholm, P. R. Edgington, P. McCabe, E. Pidcock, L. Rodriguez-Monge, R. Taylor, J. van de Streek, P. A. Wood, *J. Appl. Crystallogr.* **2008**, *41*, 466–470.
[45] A. L. Speck, *Acta Crystallogr. Sect. D* **2009**, *65*, 148–155.

